

**Microwave response of two-dimensional electron rings**

V. A. Kovalskii and S. I. Gubarev

*Institute of Solid State Physics, RAS, Chernogolovka, 142432 Russia*

I. V. Kukushkin

*Institute of Solid State Physics, RAS, Chernogolovka, 142432 Russia**and Max-Planck-Institut für Festkörperforschung, Heisenbergstrasse 1, 70569 Stuttgart, Germany*

S. A. Mikhailov

*Max-Planck-Institut für Festkörperforschung, Heisenbergstrasse 1, 70569 Stuttgart, Germany**and ITM, Electronics Design Division, Mid-Sweden University, 85170 Sundsvall, Sweden*

J. H. Smet and K. von Klitzing

*Max-Planck-Institut für Festkörperforschung, Heisenbergstrasse 1, 70569 Stuttgart, Germany*

W. Wegscheider

*Walter Schottky Institute, Technische Universität München, Am Coulombwall, D-85748 Garching, Germany*

(Received 4 January 2006; revised manuscript received 2 April 2006; published 2 May 2006)

We report microwave absorption studies on rings containing two-dimensional electrons. The absorption is measured on single rings with different widths using an optical luminescence technique. The dispersion of the plasmon modes has been determined in the presence of a perpendicular magnetic field. The transformation of two-dimensional plasmons in the disk geometry into plasmons with one-dimensional character in a narrow ring is addressed. Experimental data are compared with theoretical estimates based on a self-consistent solution of the Poisson and hydrodynamic equations.

DOI: [10.1103/PhysRevB.73.195302](https://doi.org/10.1103/PhysRevB.73.195302)

PACS number(s): 71.35.Cc, 71.30.+h

**I. INTRODUCTION**

Plasma oscillations in low-dimensional electron systems have been actively studied over the past three decades.<sup>1–4</sup> Most studies have been carried out with far-infrared transmission spectroscopy<sup>5–9</sup> and Raman scattering techniques<sup>10,11</sup> on periodic arrays of small disks (quantum dots), antidots or quantum wires. More recently, the focus of plasma-wave investigations has shifted toward much lower frequencies, the microwave regime, as well as stand-alone geometries. For instance, the microwave absorption spectrum of a single macroscopic disk was explored in Ref. 12 and of a narrow stripe in Ref. 13. These developments have been triggered by the progressive improvement in the quality of quantum-well heterostructures, which has pushed the boundary for the observability of two-dimensional plasmons ( $\omega\tau > 1$ , where  $\tau$  is the momentum relaxation time) to lower frequencies. Lower frequencies in turn imply that studies can proceed on larger-scale geometries for which it is no longer necessary to consider periodic arrays in order to enhance the sensitivity. Stand-alone geometries offer the important advantage that complications due to coupling between adjacent structures are entirely avoided. Recent studies in this low-frequency regime on single geometries already disclosed novel physics: it was shown both experimentally and theoretically that electrodynamic effects—radiative decay and retardation—substantially influence the response of these two-dimensional (2D) systems at microwave frequencies.<sup>12,14–17</sup> The discoveries of the microwave-induced zero-resistance states,<sup>18,19</sup> whose origin remains con-

troversial, as well as  $B$ -periodic photoresistance and photo-voltage oscillations<sup>20</sup> further add to the necessity of a comprehensive study of the electrodynamics and plasmon physics at microwave frequencies as this physics has been claimed to be relevant (for instance, see Ref. 21) for the microwave-induced zero resistance.

In this paper, we study the microwave response of two-dimensional electron rings. Geometrically, rings are close to disks (or dots) and wires in different limiting cases. In dots and wires the spectrum of the collective excitations is composed of two branches: the bulk mode and the edge magnetoplasmon (EMP) mode. In a strong perpendicular magnetic field  $B$ , the bulk magnetoplasmon frequency approaches the cyclotron resonance (CR) frequency  $\omega \rightarrow \omega_c$ , while the EMP frequency decreases as the magnetic field is raised. At low values of the magnetic field, the behavior of bulk and edge modes in disks and stripes is, however, different. In disks the plasmons exhibit two-dimensional character, whereas in stripes we are dealing with 1D plasmons. In circular disks, the bulk and edge magnetoplasmon modes converge to the same bulk plasmon frequency as  $B$  approaches zero. At non-zero  $B$ , this plasma resonance splits into bulk and edge branches. In wires (or in long rectangular stripes) the bulk and edge magnetoplasmon modes tend to different frequencies as  $B \rightarrow 0$ . The plasmon frequency of the upper resonance mode is inversely proportional to the square root of the width of the stripe, while the zero-field frequency of the lower mode is inversely proportional to the length of the stripe.<sup>22</sup>

The transition from 2D to 1D behavior of the magnetoplasma modes can be followed in single stripes of 2D elec-

trons with different length to width ratios,<sup>13</sup> and in elliptically shaped mesas with various ratios between the minor and major axes.<sup>23</sup> Another interesting possibility is to study this transition in ring-shaped 2D electron systems by varying the ratio of the outer ( $D$ ) and inner ( $d$ ) diameters of the ring. So far, little consideration has been given to the ring geometry except for the experiments described in Refs. 24 and 25 which mainly involved rings with an aspect ratio  $\eta \equiv d/D$  of  $\sim 1/2 - 1/4$ . The goals of this paper are the study of plasmon spectra in rings across a broader range of  $\eta$  and the investigation of the 2D to 1D plasmon transition. Rings with an aspect ratio  $d/D$  close to 1 can be viewed as narrow ring-shaped stripes and we expect 1D behavior of the plasmons whose wave number is determined by the average perimeter of the ring. In rings with  $d/D \ll 1$  the lower plasmon mode (EMP running along the outer edge of the ring) should mainly follow the EMP spectrum of a disk. The upper mode however is expected to deviate strongly from the CR line, because this mode corresponds to EMPs running around the inner perimeter of the ring.<sup>24,25</sup> Important distinctions from the previous studies are that we perform measurements in the microwave (gigahertz) frequency range about two orders of magnitude lower than the plasmon frequencies in Ref. 24 and our investigations are not performed on arrays of rings, but rather on a single-ring. Single-ring studies avoid the possible influence of inter-ring interaction on the spectra.

## II. EXPERIMENT

The measurements were carried out on a set of different mesas fabricated with photolithography from a modulation-doped GaAs/AlGaAs single quantum well with a width of 30 nm and an electron mobility  $\mu$  of approximately  $5 \times 10^6 \text{ cm}^2/\text{Vs}$ . These mesas had the shape of a ring, all with the same outer diameter  $D=1$  mm but different inner diameters ( $d=0.8, 0.6, 0.4, 0.2,$  or  $0.1$  mm), or a disk with an identical outer diameter. The 2D electron concentration was determined under the conditions of the experiment from magnetoluminescence spectra in which Landau quantization of the electron energy spectrum is resolved.<sup>26</sup> The number of fully occupied Landau levels and its variation with magnetic field allows us to reliably extract the electron density. This method was for instance applied to the disk device, in which the determination of the plasma frequency yields an alternative approach to determine the density. The density extracted from the magnetoluminescence measurements and from a measurement of the plasma frequency deviated by less than 5%. The electron density in the various structures varied from  $1.1 \times 10^{11}$  to  $1.4 \times 10^{11} \text{ cm}^{-2}$ .

The spectra of the dimensional magnetoplasma resonances were measured with a sensitive optical scheme geared toward the detection of resonant absorption of microwave radiation.<sup>27</sup> This technique relies on the comparison of the luminescence spectrum of the two-dimensional electron gas obtained in the absence of microwave radiation with the spectrum acquired when microwave radiation is incident on the sample. A stabilized semiconductor laser provided the continuous wave excitation for the luminescence measurements. Its light with a wavelength of 750 nm was guided to

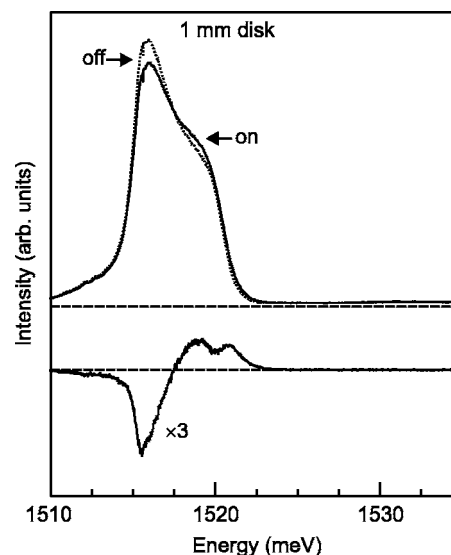


FIG. 1. Luminescence spectra obtained on a disk geometry with a diameter of 1 mm with and without microwave radiation present (upper curves). The corresponding differential spectrum is shown at the bottom. The incident radiation has a frequency of 6 GHz. The magnetic field is chosen so that a resonance occurs ( $B=105$  mT). The electron concentration is  $1.4 \times 10^{11} \text{ cm}^{-2}$ .

the sample with a 0.4 mm diameter quartz optical fiber mounted perpendicular to the sample at a distance of approximately 1 mm to ensure illumination of the entire device. The fiber was also used to collect the luminescence signal that appeared as a result of recombination. The optical signal was analyzed with a double-grating spectrometer with a spectral resolution of 0.03 meV and a charge-coupled device camera. An HP-83623B generator supplied the microwave radiation with frequencies up to 20 GHz. A coaxial cable suitable for transmission of frequencies up to 20 GHz and with an attenuation of less than 5 dB was used to guide the microwave radiation to the sample. The exposed inner conductor near the end of the coaxial line served as a dipole antenna. Approximately 10 mW of radiation was sent down the coaxial line; however, most of this power is reflected due to a lack of impedance matching at the end of the line. Figure 1 illustrates a typical radiation recombination spectrum of the 2D electrons in the presence and absence of microwave radiation (upper curves) as well as the corresponding differential spectrum (lower curve). The spectra were obtained at 4.2 K for a disk structure with an electron concentration of  $1.4 \times 10^{11} \text{ cm}^{-2}$  when a resonance occurs:  $f=6$  GHz and  $B=105$  mT. At resonance, the electronic system heats up and electrons redistribute near the Fermi surface. Hence, the luminescence intensity changes for energies near the Fermi energy. After recording the luminescence spectrum with and without microwave radiation present, the differential spectrum was calculated. The absolute value of this difference signal was integrated over the recorded spectral range. The resulting value served as a measure of the microwave absorption strength. Its magnetic-field dependence was then studied at different excitation frequencies.

### III. THEORY

The ring problem has been treated theoretically by Zaremba<sup>28</sup> as well as Reboredo and Proetto<sup>29</sup> in the context of the experiment reported in Ref. 24. The disk problem has been addressed by Fetter in Ref. 30. These authors solved the Poisson and hydrodynamic equations self-consistently. We perform in essence the same type of calculations, but take also into account specific features of the problem which arise for long-wavelength, low- (microwave-) frequency excitation. Retardation effects<sup>12</sup> are neglected. Estimates show that they are not so important at the electron densities typical for our experiments.

To calculate the spectrum of plasma modes in rings, we solve the following Poisson and hydrodynamic equations:

$$\Phi_L(x) + \int_{\eta}^1 x' dx' K_L(x, x') N_L(x') = 0, \quad (1)$$

$$(\Omega^2 - \Omega_c^2) N_L(x) = \left[ \frac{1}{x} \frac{\partial}{\partial x} \left( x \frac{\partial}{\partial x} \right) - \frac{L^2}{x^2} \right] \Phi_L, \quad (2)$$

with the boundary conditions

$$\left( \frac{d\Phi_L}{dx} + L \frac{\Omega_c \Phi_L}{\Omega x} \right)_{x=1, \eta} = 0 \quad (3)$$

at the internal ( $x \equiv r/R = \eta$ ) and external ( $x=1$ ) boundaries of the ring (compare with Ref. 30). Here  $\Phi_L$  and  $N_L$  are the (dimensionless) plasmon potential and the density,  $L=|l|$ ,  $\Omega = \omega/\omega_0$ ,  $\Omega_c = (\omega_c/\omega_0) \text{sgn}l$ , and

$$\omega_0^2 = \frac{4\pi n_s e^2}{mD}. \quad (4)$$

It is assumed that the 2D electron gas is located on the surface of a finite-thickness semiconductor substrate. The kernel  $K_L(x, x')$  of the integral equation (1) reduces to

$$K_L(x, x') = \int_0^{\infty} \frac{J_L(qx) J_L(qx') dq}{\Delta(\kappa, 2qh/D)}, \quad (5)$$

$$\Delta(\kappa, 2qh/D) = \frac{1}{2} \left( 1 + \kappa \frac{1 + \kappa \tanh 2qh/D}{\tanh 2qh/D + \kappa} \right), \quad (6)$$

and takes into account screening of the electrostatic field. Here,  $\kappa$  and  $h$  are the dielectric constant and the thickness of the substrate (GaAs),  $J_L$  are Bessel functions, and the variables  $x$ ,  $x'$ ,  $q$  are dimensionless. Notice that at microwave frequencies (here 0–20 GHz), it is not appropriate to consider a semi-infinite semiconductor substrate, as was usually done at far-infrared frequencies. The wavelength of the microwave radiation ( $\sim 1$  cm) typically exceeds the substrate thickness ( $\sim 0.5$  mm), so that a more realistic description of the dielectric environment is essential.

We solve the problem (1) and (3) by expanding the potential  $\Phi_L$  in a complete orthonormal set of functions [combinations of Bessel functions  $J_L$  and  $Y_L$  satisfying the boundary conditions (3)], and by reducing (1) and (2) to a matrix eigenvalue problem. The size of the matrix is chosen sufficiently large to ensure that calculations converge. In the fol-

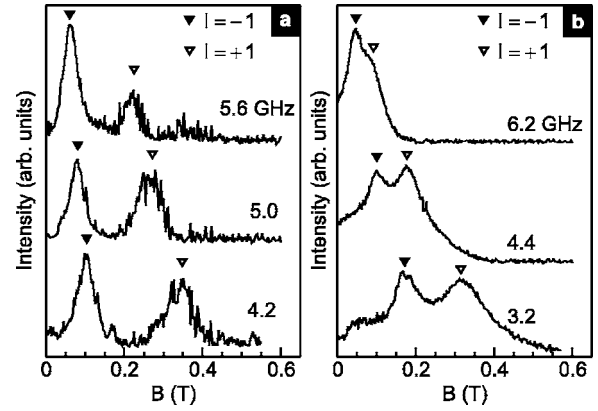


FIG. 2. Typical magnetic-field dependencies of the absorption amplitude for the indicated microwave radiation frequencies. Data are shown for two ring-shaped mesas with the following dimensions: (a)  $D=1$  mm,  $d=0.4$  mm and (b)  $D=1$  mm,  $d=0.6$  mm. The electron concentration in these rings is  $1.25 \times 10^{11}$  (a) and  $1.15 \times 10^{11}$  cm<sup>-2</sup> (b). The observed modes are  $n=0$  modes.

lowing section, we compare the results of our calculations with the experimental data.

### IV. RESULTS AND DISCUSSION

Figure 2 illustrates typical scans of the absorption amplitude as a function of the magnetic field at several microwave frequencies for two rings with the outer diameter  $D$  equal to 1 mm and the inner diameters  $d=0.4$  and 0.6 mm. The arrows mark the magnetoplasma modes observed in these rings. The modes are characterized by two quantum numbers, the radial quantum number  $n=0, 1, \dots$  and the azimuthal quantum number (angular momentum)  $l=0, \pm 1, \dots$ <sup>24,25</sup> The magnetoplasma resonances with  $n=0$  and  $l=\pm 1$  dominate in all absorption spectra as they possess the largest oscillator strength.

The  $B$ -field dependence of the magnetoplasma resonance frequencies for rings with the same outer diameter  $D=1$  mm but different inner diameters  $d$  of 0.2, 0.6, and 0.8 mm are plotted in Figs. 3(b)–3(d). For comparison, we also show the magnetoplasma spectrum of a disk-shaped mesa with  $D=1$  mm in Fig. 3(a). Even though rings and disks share the same symmetry properties and their resonance modes are classified with the same quantum numbers, there are pronounced changes in the spectrum as the disk geometry [Fig. 3(a)] is replaced with a narrow ring geometry [Figs. 3(b)–3(d)]. The most striking difference is the behavior of the mode with  $n=0$  and  $l=+1$ , which we will refer to as the  $\omega_{0+}$  branch. Both in the disk [Fig. 3(a)] and in the broad ring with the aspect ratio  $d/D=0.2$  [Fig. 3(b)], this mode exhibits a positive dispersion at low magnetic fields, and hence the usual behavior of a bulk magnetoplasmon. Conversely, in narrow rings with an aspect ratio  $d/D$  larger than  $1/2$  [Figs. 3(c) and 3(d)], the  $\omega_{0+}$  branch develops a negative dispersion in the field range where this mode is observed. Its frequency decreases monotonically with increasing magnetic field. This negative dispersion is similar to the dispersion of the lower  $\omega_{0-}$  branch, i.e., the  $n=0$ ,  $l=-1$

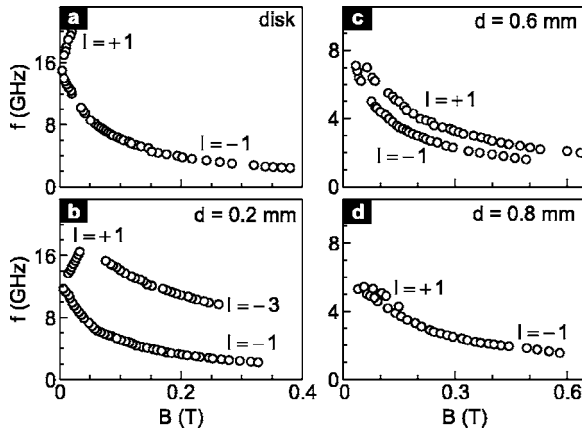


FIG. 3. The resonance frequencies of  $n=0$  magnetoplasma modes in disk and ring geometries. The outer diameter  $D$  of the disk (a) and rings (b)–(d) is 1 mm. The inner diameter  $d$  of the rings has been indicated on each panel where it has relevance. The electron densities were as follows:  $1.4 \times 10^{11}$  (a),  $1.1 \times 10^{11}$  (b), (c), and  $1.2 \times 10^{11} \text{ cm}^{-2}$  (d).

mode. These excitations are related to plasma oscillations propagating along the outer and inner boundaries of the rings. They become localized near the edges at sufficiently large magnetic-field values.<sup>24,25</sup> The  $\omega_{0-}$  mode corresponds to the EMP at the outer edge, while the  $\omega_{0+}$  mode comprises an EMP localized at the inner edge of the ring. In addition to these fundamental modes, in some instances [Fig. 3(b)] we also observe the mode with  $l=-3$ .

Figure 4 shows the calculated spectra of the plasmons in disk and ring geometries with the same parameters as those for which the experimental data are shown in Fig. 3. Qualitative agreement between experiment and theory is apparent. Theory properly predicts a change of the slope for the  $\omega_{0+}$  branch from positive to negative away from  $B=0$  as the as-

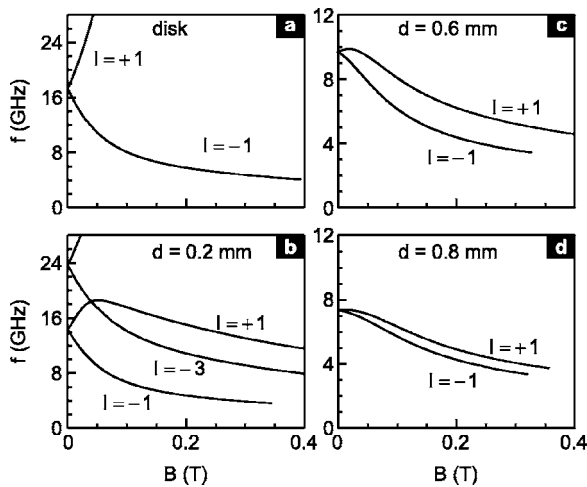


FIG. 4. Calculated magnetoplasma frequencies of the modes with quantum numbers  $(n, l) = (0, \pm 1)$  and  $(0, -3)$  for disk and ring geometries as in Fig. 3 (outer diameter  $D=1$  mm in all cases;  $d$  is indicated in panels where it is relevant). The electron densities are as in Fig. 3:  $1.4 \times 10^{11}$  (a),  $1.1 \times 10^{11}$  (b), (c), and  $1.2 \times 10^{11} \text{ cm}^{-2}$  (d). The substrate thickness was assumed to be 0.4 mm.

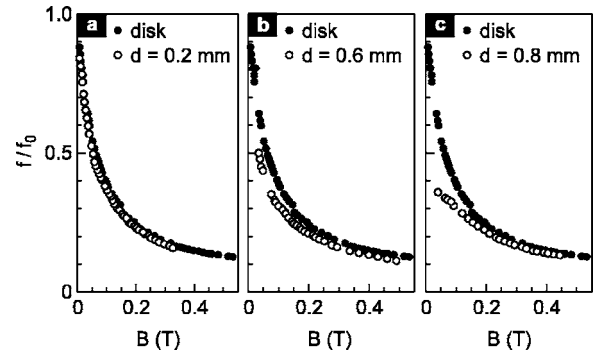


FIG. 5. A comparison between the  $\omega_{0-}$  branch of the disk geometry with the  $\omega_{0-}$  resonance frequencies of one of the three rings under study: (a) wide ring with  $d/D=0.2$  and  $n_s=1.1 \times 10^{11} \text{ cm}^{-2}$ , (b) intermediate ring with  $d/D=0.6$  and  $n_s=1.15 \times 10^{11} \text{ cm}^{-2}$ , and (c) narrow ring with  $d/D=0.8$  and  $n_s=1.2 \times 10^{11} \text{ cm}^{-2}$ . The outer diameter  $D$  equals 1 mm for all geometries. The resonance frequencies are normalized to the plasma frequency  $f_0$  (see text) of a disk with the same outer diameter (1 mm) and electron density.

pect ratio  $d/D$  increases. For  $d/D$  exceeding 0.6 the dispersion also flattens as  $B \rightarrow 0$  in accordance with experimental findings. Quantitatively, the theoretical and experimental curves for the disk [Figs. 3(a) and 4(a)] agree quite well—a 6% reduction of the experimental frequencies as compared to the theoretical frequencies can likely be explained by the weak influence of retardation, which has not been included in the theory. For rings, a bigger discrepancy is observed between experiment and theory. The experimental data points lie systematically below the theoretical ones. The difference amounts to 10–20%. The reason for this discrepancy is not known at present. It is worth noting that the difference between theory and experiment was substantially smaller in samples with electron densities twice as large.<sup>25</sup> The growing discrepancy between experiment and theory in low-density samples might point to a larger influence of electron-electron interaction.

Differences between the magnetoplasma spectra of ring- and disk-shaped structures are not restricted to the upper resonance mode  $\omega_{0+}$ . The dispersion of the lower resonance mode  $\omega_{0-}$  propagating along the outer boundary of the ring also undergoes changes as we switch from a disk to a ring geometry. To highlight these modifications, it is instrumental to replot the data of Fig. 3 and normalize for the variations in the electron density. For the three rings in Figs. 3(b)–3(d), the lower branch is compared with the disk data of Fig. 3(a) in Fig. 5. The resonance frequencies observed in each ring were normalized by dividing through the plasma frequency  $f_0$  of a disk with the same electron density  $n_s$  and outer diameter:  $2\pi f_0 = (4\pi n_s e^2 / m \bar{\epsilon} D)^{1/2}$ . Here,  $\bar{\epsilon} = (1 + \kappa)/2$  is the average dielectric constant of free space and GaAs. For the wide ring with  $d=0.2$  mm, Fig. 5(a) displays no significant modifications in the  $B$ -field dependence of the  $\omega_{0-}$  mode. Even for the ring with  $d=0.6$  mm in Fig. 5(b), the frequency of the outer EMP remains almost unchanged on the high-magnetic-field side. It drops by about 20% of the plasma frequency in the disk as one approaches  $B=0$ . This behavior can be accounted for by the interaction among the  $\omega_{0-}$  and  $\omega_{0+}$  modes. The localization at large magnetic fields of the

magnetoplasma oscillations at the ring boundary suppresses this interaction, whereas near  $B=0$  these modes are not localized. The interaction between both modes is weaker in rings with smaller aspect ratios. These trends are evident from a comparison of Figs. 5(a)–5(c). The plasma frequency in the narrow ring [Fig. 5(c)] for instance is almost three times smaller than the plasma frequency in the disk with the same electron concentration ( $f/f_0 \sim 0.4$ ) and the magnetic-field dependence is much weaker than that in the disk. In the EMP regime at larger fields ( $B > 200$  mT), the disk and ring resonance curves merge again.

When studying the properties of the magnetoplasmons of narrow rings, it should be kept in mind that these ought to resemble those in a 1D electron system (e.g., narrow stripes or wires). The low-frequency collective excitations of 2D electrons confined to a stripe were considered theoretically in Ref. 22 (see also Ref. 31). For a long and narrow stripe with a half-width of  $a$ , the energy spectrum of magnetoplasmons when adopting a semielliptical electron density profile reduces to

$$\omega^2(k) = \frac{\Omega_0^2 k^2 a^2}{2} \frac{\Omega_0^2}{\Omega_0^2 + \omega_c^2} \ln\left(\frac{4}{|k|ae^\gamma}\right) \quad (7)$$

for small wave vectors  $k$  ( $ka \ll 1$ ). Here,  $\omega_c$  is the cyclotron frequency,  $\gamma \approx 0.577\dots$  is the Euler constant, and

$$\Omega_0 = \left(\frac{8n_s e^2}{m\bar{\epsilon}a}\right)^{1/2} \quad (8)$$

is the plasma frequency of the transverse mode describing a charge density oscillation across the stripe. Equation (7) can be rewritten in the following form:

$$\frac{1}{\omega^2(k)} = \left(\frac{1}{\Omega_0^2} + \frac{\omega_c^2}{\Omega_0^4}\right) \beta^{-1}, \quad (9)$$

where

$$\beta = \frac{k^2 a^2}{2} \ln\left(\frac{4}{|k|ae^\gamma}\right). \quad (10)$$

According to Eq. (9), for the 1D magnetoplasma mode with frequency  $f$  in a narrow stripe,  $1/f^2$  obeys a linear relationship when plotted versus  $B^2$ . It is worthwhile to regard the mode in a narrow ring as a 1D plasmon in a stripe with an effective half-width  $a^* = (D-d)/4$  and an effective length  $l^*$  equal to the mean perimeter of the ring  $l^* = \pi(D+d)/2$ . Certainly the expression (7) for a stripe cannot be directly applied to the ring geometry for a number of reasons. In a ring shape the induced charge configuration and currents will be different compared with a stripe. Also, the electron density distribution in any realistic device deviates considerably from the semielliptical profile assumed in Ref. 22. The density profile is much closer to a step function. The density is constant almost everywhere within the mesa except for a narrow region near the mesa boundary where it drops to zero. Both disparities strongly affect the values of  $\Omega_0$  and  $\beta$ . Hence, we will use  $\Omega_0$  and  $\beta$  as fitting parameters. To make the distinction with the theoretical values we will refer to these fit parameters as  $2\pi F_0^{\text{expt}}$  and  $\beta^{\text{expt}}$ . A fit of Eq. (7) to

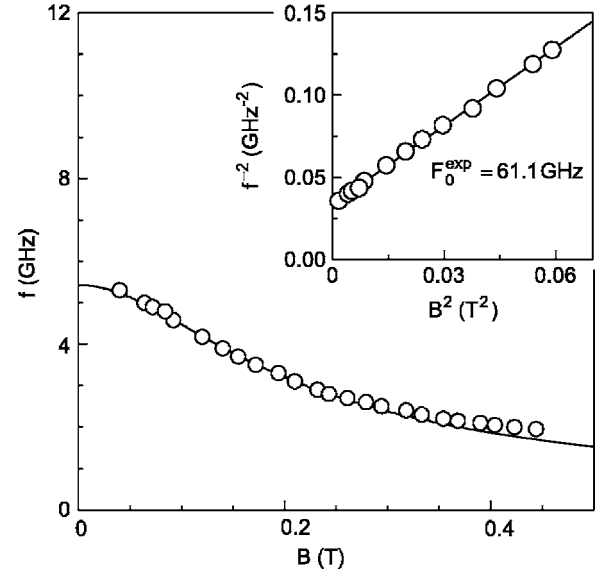


FIG. 6. The magnetic-field dependence of the  $\omega_{0-}$  mode of the narrow ring with  $D=1$  mm,  $d=0.8$  mm, and the density  $n_s=1.2 \times 10^{11}$  (hollow dots). The solid line has the functional form described by Eq. (9). The values of  $\beta^{\text{expt}}$  and  $F_0^{\text{expt}}$  were obtained from a least-squares fit to the data. The inset shows the same data and fit but  $f^{-2}$  is plotted versus  $B^2$ .

the experimental data for the narrow ring with  $D=1$  mm and  $d=0.8$  mm is displayed in the inset of Fig. 6. The  $B$ -field dependence of the 1D magnetoplasmon is indeed well described by a linear law when plotting  $f^{-2}$  as ordinate and  $B^2$  as abscissa. From this fit to the data, we find a value of 61.1 GHz for the transverse plasma frequency  $F_0^{\text{expt}}$ . This is in good qualitative agreement with the value obtained from the modified formula (8) taking into account the ring shape [where we substitute  $a^* = (D-d)/4$  for  $a$ ]. It yields  $\Omega_0/2\pi = 51.6$  GHz instead. The other fit parameter  $\beta^{\text{expt}}$  converges to 0.008 and is less consistent with the value calculated from Eq. (10):  $\beta=0.018$ . Figure 6 also plots the experimental data for the  $\omega_{0-}$  mode and the calculated frequencies using the fitted values  $\beta^{\text{expt}}$  and  $F_0^{\text{expt}}$  in the usual coordinates  $f$  and  $B$  from which we also conclude that Eq. (9) captures well the magnetic-field-dependent behavior.

In Fig. 7 the zero-field plasma frequency  $\omega_{0-}(B=0)$  is plotted as a function of the aspect ratio  $\eta=d/D$  for six different rings. The density ranged from  $1.1 \times 10^{11}$  to  $1.4 \times 10^{11}$   $\text{cm}^{-2}$ . The frequencies were normalized to the zero-field plasma frequency  $f_0$  in a disk with the same outer diameter and density in order to allow a comparison despite differences in the density. Also included in this plot are theoretical values for the zero-field plasma frequencies of rings based on the theory described in Sec. III (open circles). The discrepancy of 10–15% between theory and experiment has been pointed out and discussed previously. Here we mainly wish to compare with values extracted from Eq. (7) by substituting  $ka$  with  $(2\pi/l^*)a^* = (D-d)/(D+d)$  and taking  $\omega_c$  equal to zero (see solid curve in Fig. 7). For narrow rings and for rings with intermediate values of  $d/D$ , the curve calculated with formula (7) nearly coincides with the open circles. Deviations start to occur for small aspect ratios. This should

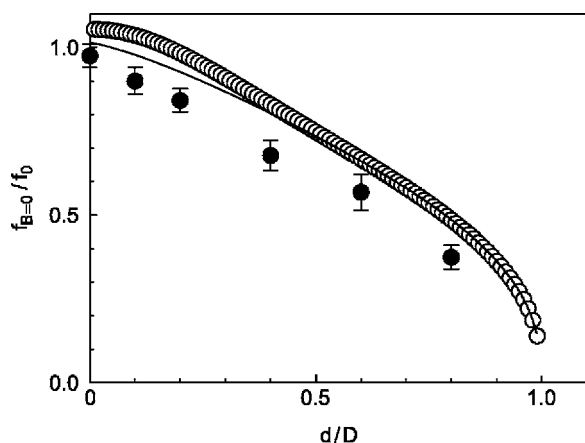


FIG. 7. The zero-field plasma frequency  $f_{B=0}$  for the ring geometry as a function of the aspect ratio  $\eta=d/D$ . Frequencies are normalized to the zero-field plasma frequency  $f_0$  of a disk with the same outer diameter and density. The electron density of the rings that contributed the experimental data points (solid circles) to this plot varied from  $1.1 \times 10^{11}$  to  $1.4 \times 10^{11}$   $\text{cm}^{-2}$ . Open circles are theoretical estimates obtained from the self-consistent solution of the Poisson and hydrodynamic equations as described in Sec. III. The solid curve corresponds to the resonance frequency predicted from Eq. (7) for  $B=0$ .

not come as a surprise since Eq. (7) assumes a narrow stripe-like geometry. Hence, it loses its validity as we approach the disk geometry.

It is interesting to compare the velocities of 1D plasmons in a long and narrow stripe with those in a narrow ring with the same width and 2D electron concentration. On a stripe of 0.1 mm width with an electron density of  $1.2 \times 10^{11}$   $\text{cm}^{-2}$ , a velocity  $v_{1D}$  of  $1.82 \times 10^7$  m/s has been measured.<sup>13</sup> In the narrow ring with  $D=1$  mm and  $d=0.8$  mm and the same electron density, we can estimate the 1D plasmon velocity at

zero magnetic field as  $v_{1D}=\pi\left(\frac{d+D}{2}\right)f(B=0)$ . Since for this ring we found  $f(B=0)=5.5$  GHz, the velocity equals  $v_{1D}=1.55 \times 10^7$  m/s. This is not far off from the velocity in a stripe. In general, we observe a systematic reduction of the 1D plasmon velocity in rings of approximately 15–20%. This difference presumably originates from the alterations in the current and field distributions.

## V. CONCLUSIONS

In summary, we have studied the properties of collective excitations in 2D electron rings by employing an optical method to detect the resonant absorption of microwaves. We have specifically investigated the transition from 2D to 1D magnetoplasmon behavior by measuring a set of rings with the same outer diameter and electron density, but different inner diameter. It has been shown that the change from a disk geometry to a narrow ring shape produces significant changes in the magnetic field dispersion as well as absolute value of the plasmon frequencies. These experimental findings are qualitatively recovered in calculations of the disk and ring geometries. The experimental results on a narrow ring have also been analyzed in the context of theoretical predictions for 1D plasma excitations in a stripe.<sup>22</sup> From this analysis, it was possible to estimate the frequency of the  $n=1$  plasmon mode, which is associated with radial oscillations of the electron density in the ring.

## ACKNOWLEDGMENTS

We gratefully acknowledge financial support from Max-Planck and Humboldt Research Grants, the Russian Fund of Fundamental Research, INTAS, the BMBF through a young investigator award, the DFG, the Swedish Research Council, and the Swedish Foundation for International Cooperation (STINT).

<sup>1</sup>T. N. Theis, *Surf. Sci.* **98**, 515 (1980).

<sup>2</sup>D. Heitmann, *Surf. Sci.* **170**, 332 (1986).

<sup>3</sup>D. Heitmann and J. P. Kotthaus, *Phys. Today* **46**(6), 56 (1993).

<sup>4</sup>C. Schüller, in *Festkörperprobleme/Advances in Solid State Physics*, edited by B. Kramer (Vieweg, Braunschweig, 1998), Vol. 38, p. 167.

<sup>5</sup>S. J. Allen, Jr., H. L. Stormer, and J. C. M. Hwang, *Phys. Rev. B* **28**, 4875 (1983).

<sup>6</sup>T. Demel, D. Heitmann, P. Grambow, and K. Ploog, *Phys. Rev. Lett.* **66**, 2657 (1991).

<sup>7</sup>C. Dahl, J. P. Kotthaus, H. Nickel, and W. Schlapp, *Phys. Rev. B* **46**, 15590, (1992).

<sup>8</sup>K. Kern, D. Heitmann, P. Grambow, Y. H. Zhang, and K. Ploog, *Phys. Rev. Lett.* **66**, 1618 (1991).

<sup>9</sup>K. Bollweg, T. Kurth, D. Heitmann, V. Gudmundsson, E. Vasiladou, P. Grambow, and K. Eberl, *Phys. Rev. Lett.* **76**, 2774 (1996).

<sup>10</sup>A. R. Goni, A. Pinczuk, J. S. Weiner, J. M. Calleja, B. S. Dennis, L. N. Pfeiffer, and K. W. West, *Phys. Rev. Lett.* **67**, 3298

(1991).

<sup>11</sup>E. Ulrichs, G. Biese, C. Steinebach, C. Schuller, D. Heitmann, and K. Eberl, *Phys. Rev. B* **56**, R12760 (1997).

<sup>12</sup>I. V. Kukushkin, J. H. Smet, S. A. Mikhailov, D. V. Kulakovskii, K. von Klitzing, and W. Wegscheider, *Phys. Rev. Lett.* **90**, 156801 (2003).

<sup>13</sup>I. V. Kukushkin, J. H. Smet, V. A. Koval'skii, S. I. Gubarev, K. von Klitzing, and W. Wegscheider, *Phys. Rev. B* **72**, 161317(R) (2005).

<sup>14</sup>I. V. Kukushkin, D. V. Kulakovskii, S. A. Mikhailov, J. H. Smet, and K. von Klitzing, *JETP Lett.* **77**, 497 (2003).

<sup>15</sup>S. A. Mikhailov and N. A. Savostianova, *Phys. Rev. B* **71**, 035320 (2005).

<sup>16</sup>S. A. Mikhailov, *Phys. Rev. B* **70**, 165311 (2004).

<sup>17</sup>S. A. Mikhailov and N. A. Savostianova, cond-mat/0603431 (unpublished).

<sup>18</sup>R. G. Mani, J. H. Smet, K. von Klitzing, V. Narayanamurti, W. B. Johnson, and V. Umansky, *Nature (London)* **420**, 646 (2002).

<sup>19</sup>M. A. Zudov, R. R. Du, L. N. Pfeiffer, and K. W. West, *Phys.*

- Rev. Lett. **90**, 046807 (2003).
- <sup>20</sup>I. V. Kukushkin, M. Yu. Akimov, J. H. Smet, S. A. Mikhailov, K. von Klitzing, I. L. Aleiner, and V. I. Falko, Phys. Rev. Lett. **92**, 236803 (2004).
- <sup>21</sup>S. A. Studenikin, M. Byszewski, D. K. Maude, M. Potemski, A. S. Sachrajda, M. Hilke, L. N. Pfeiffer, and K. W. West, cond-mat/0602079 (unpublished).
- <sup>22</sup>I. L. Aleiner, Donxiao Yue, and L. I. Glazman, Phys. Rev. B **51**, 13467 (1995).
- <sup>23</sup>C. Dahl, F. Brinkop, A. Wixforth, J. P. Kotthaus, J. H. English, and M. Sundaram, Solid State Commun. **80**, 673 (1991).
- <sup>24</sup>C. Dahl, J. P. Kotthaus, H. Nickel, and W. Schlapp, Phys. Rev. B **48**, 15480 (1993).
- <sup>25</sup>S. I. Gubarev, V. A. Koval'skii, D. V. Kulakovskii, I. V. Kukushkin, M. N. Khannanov, J. H. Smet, and K. von Klitzing, JETP Lett. **80**, 124 (2004).
- <sup>26</sup>I. V. Kukushkin and V. B. Timofeev, Adv. Phys. **45**, 147 (1996).
- <sup>27</sup>B. M. Ashkinadze and V. I. Yudson, Phys. Rev. Lett. **83**, 812 (1999).
- <sup>28</sup>E. Zaremba, Phys. Rev. B **53**, R10512 (1996).
- <sup>29</sup>F. A. Reboredo and C. R. Proetto, Phys. Rev. B **53**, 12617 (1996).
- <sup>30</sup>A. L. Fetter, Phys. Rev. B **33**, 5221 (1986).
- <sup>31</sup>J. A. Stratton, *Electromagnetic Theory* (McGraw-Hill, New York, 1941), Sec. 9.15.